Interactions between chloramphenicol, carrier polymers and bacteria – implications for designing electrospun drug delivery systems countering wound infection

Liis Preem[a], Mohammad Mahmoudzadeh[b], Marta Putrins[c], Andres Meos[a], Ivo Laidmäe[a], Tavo Romann[d], Jaan Aruväli[e], Riinu Härmas[d], Artturi Koivuniemi[b], Alex Bunker[b], Tanel Tenson[c], Karin Kogermann[a,*]

[a]Institute of Pharmacy, University of Tartu, Nooruse 1, 50411 Tartu, Estonia

[b]Drug research program, Division of Pharmaceutical Biosciences, Faculty of Pharmacy, University of Helsinki, P.O. Box 56, FI-00014 Helsinki, Finland

[c]Institute of Technology, University of Tartu, Nooruse 1, 50411 Tartu, Estonia

[d]Institute of Chemistry, University of Tartu, Ravila 14a, 50411, Tartu, Estonia

[e]Institute of Ecology and Earth Sciences, University of Tartu, Ravila 14a, 50411, Tartu, Estonia

*Correspondence to: Karin Kogermann (Telephone: +372 737 5281; Fax: +372 737 5289). E-mail address: karin.kogermann@ut.ee (K. Kogermann).

1. Materials and Methods

1.1 Preparation of physical mixtures and an amorphous form of chloramphenicol (CAM)

For the solid state characterization of drug within fibers, physical mixtures and amorphous CAM were prepared. To prepare PCL powder from pellets, it was first melted to obtain filaments and these filaments were consecutively mechanically crushed with a pestle in a mortar together with liquid nitrogen. The powder was sieved through 500 μm sieve. Physical mixtures of PCL:CAM (24:1), PCL:PEO (5:1) and PCL:PEO:CAM (20:4:1) were prepared by mixing the powdered substances in a mortar with a pestle using geometric dilution. The ratios of the substances matched those in electrospun fibers. Amorphous CAM was prepared from the crystalline form by quench cooling of the melt. Briefly, the powder was melted on a hotplate, followed by a rapid cooling with liquid nitrogen. The glassy material formed was gently powdered with pestle in a mortar. Samples were analyzed immediately after preparation.

1.2 Computational methods

The parametrization of PCL, PEO and CAM molecules was carried out using the all-atom optimized potentials for liquid simulation (OPLS-AA) force field.[1] The validation of OPLS-AA parameters for PEO has already been carried out in our group[2] and for PCL, this has already been performed by Pasquale et al.[3] For the case of CAM, there are three kinds of dihedrals not parametrized in the OPLS-AA force field. We parametrized these dihedrals using the B3LYP functional and the aug-cc-pvtz basis set using the Gaussian 09 package.[4] Following full optimization of the structure of CAM using B3LYP/aug-cc-pvtz, all partial atomic charges of CAM were derived from a least-squares fit of the electrostatic potential through a Merz-Kollman scheme.[5] The obtained charges were then converted into restrained electrostatic potential (RESP) charges[6] using the Antechamber module[7] of the Amber14[8] suite

of programs. All partial charges and dihedral parameters for CAM are included in a molecular topology (file clp.itp) and the atom types in the model are shown in Fig. S1. The corresponding OPLS parameters were used for all ions and the deionized water as solvent was modelled using the simple point charge (SPC/E) potential.[9]

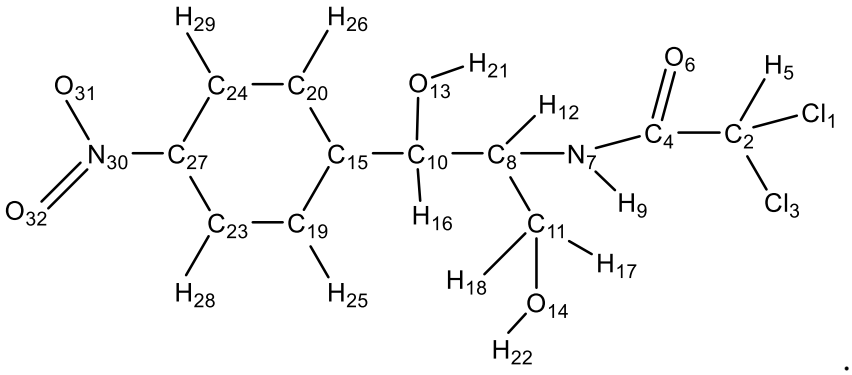

Fig. S1 Atom types used in the CAM topology, ITP file of the molecule is also included as Supporting Information.

All simulations were carried out at physiological ionic strength of 145 mM produced through the addition of Na^+ and Cl^- ions to the simulation box. The number of each type of molecule/ion in the simulation is shown in Table 1 in the main text.

Following solvation of the systems, the potential energy of the systems was minimized through the steepest descent method using 50 000 minimization steps. Following this, an initial equilibrium configuration for each system was achieved through first simulation at constant volume and a temperature for 100 ps (NVT ensemble). The V-rescale thermostat (12) with a coupling constant of 0.1 ps-1 was utilized to maintain a constant temperature of 310 K during all NVT simulations. After this, all systems were simulated for 100 ns under constant pressure and temperature conditions (NPT) with the V-rescale thermostat and the Parrinello-Rahman barostatat with coupling constants of 0.1 and 2.0 ps-1 respectively. A time step of 2 fs was used in all cases. The cut-off for the Lennard-Jones interactions was set to 10

Å. The particle mesh Ewald (PME) method[10] was used to calculate long-range electrostatic effects with a real space cut-off of 10 Å and the LINCS algorithm[11] was used to constrain all bond lengths. For all simulation trajectories, the coordinates of the atoms were saved every 10 ps in the trajectory files and analyzed using analysis tools present within the GROMACS simulation package. All electrostatic potential maps were created using the Molden program[12] and the VMD visualization package[13] was used to render all images of the simulated systems. All solvent accessible surface area (SASA) calculations were made using the Naccess program.[14]

1.3 Preparation of DMSO stocks of bacteria

For preparing DMSO stocks of these bacteria overnight liquid cultures were diluted 1:100 in fresh Lysogeny broth (LB) and grown aerobically to exponential phase. At an optical density at 600 nm of 0.8, dimethyl sulfoxide (DMSO) was added to a final concentration of 8% and the cultures were immediately frozen in 120 µl aliquots at -80 °C. Stocks were stored up to 6 months.

2. Results

2.1 Drug-carrier polymer interactions

Table S1. Characteristic infrared bands of PCL[15–18], PEO[19,20] and CAM[21,22]

	Assignments	**Wavenumber (cm^{-1})**
PCL	$'v_{as}(CH_2)$	2994 (amorphous)
	$v_s(CH_2)$	2865 (crystalline)
	v(C=O)	1731(amorphous), 1724 (crystalline)
	v(C-O C-C)	1295 (crystalline), 1157 (amorphous)
	v_{as}(COC)	1245 (crystalline)

	ν(OC-O)	1192 (crystalline)
	ν_s(COC)	1170
	ν(COC)	1107
	γ_{in} (CH_2)	731 (crystalline)
	γ_{out} (CH_2)	710 (crystalline)
PEO	ν_{as}(CH_2)	2946
	ν_s(CH_2)	2886
	ω(CH_2)	1361, 1343
	τ(CH_2)	1281, 1242
	ν(COC)	1145 (crystalline), 1095 (crystalline), 1059 (crystalline)
	ρ(CH_2)	963, 843
CAM	ν(C=O)	1686
	ring stretch	1563
	ν_{as}(NO_2)	1520
	ν_{as}(C-Cl)	817
	ring deformation	643

Key: PCL – polycaprolactone; PEO – polyethylene oxide; CAM – chloramphenicol.

2.2 Thermal behavior

Interestingly, no CAM melting endotherm is present in physical mixtures (Fig. S2). As both carrier polymers melt at relatively low temperatures (PCL between 59-64 °C[23] and PEO between 68-74 °C[24,25]) and CAM at much higher temperature (150.5-151.5 °C), it is possible that in physical mixtures crystalline CAM dissolves in molten polymer(s) before having a chance to melt. As the drug in the electrospun fibers is in an amorphous state, suggested by XRD and ATR-FTIR, no melting endotherm is observed.

The addition of PEO changed the thermal behavior of electrospun fibrous mats. In physical mixtures of PCL and PEO, two distinct melting endotherms at 60.7 and 69.4 °C were present, but in fibers with the same composition PEO melting endotherm shifted to lower temperatures and appeared as a shoulder on PCL melting endotherm (Table 1). This behavior has been also shown previously.[26] For the case of PCL/PEO/CAM physical mixtures, again two melting endotherms same as with PCL/PEO physical mixtures appeared, but with the fibers only one melting endotherm at 58.5 °C was seen. The PCL/CAM fibers exhibit a melting point at 57.7 °C, whereas the corresponding physical mixtures show PCL melting endotherm at 60.1 °C. These changes indicate possible interactions between PCL, PEO and CAM molecules in electrospun fibers, as also proposed by ATR-FTIR.

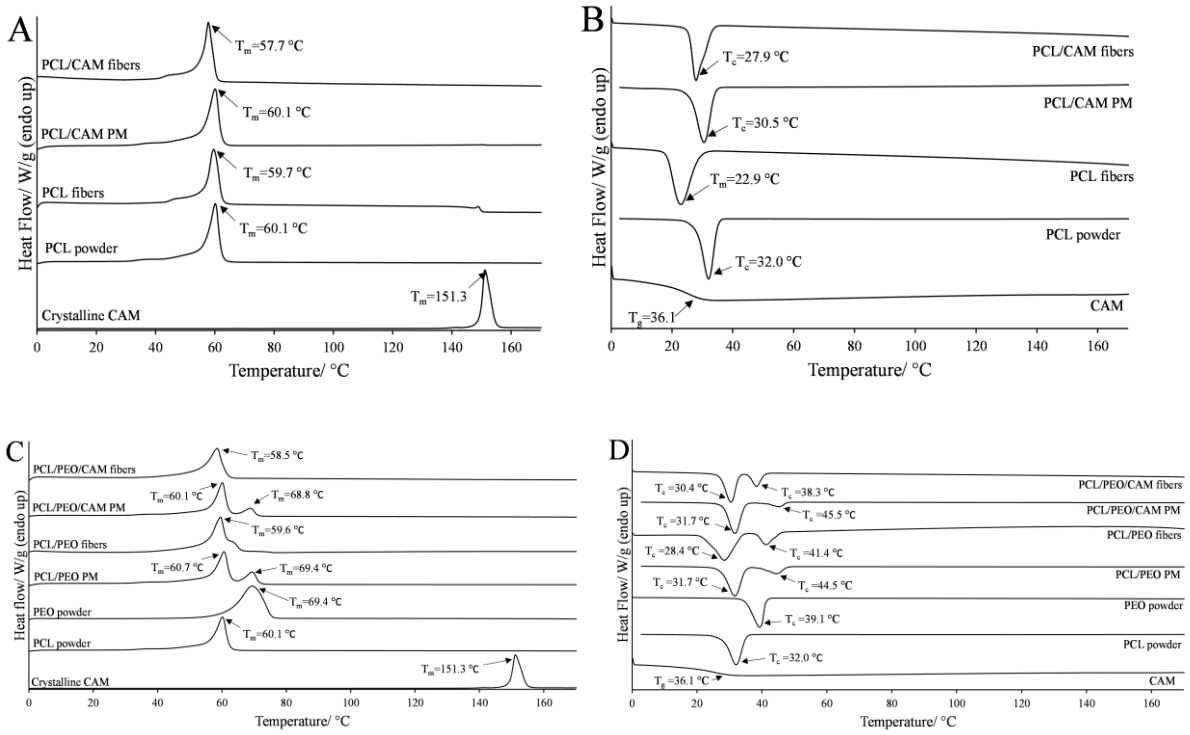

Fig. S2 Differential scanning calorimetry **(**DSC) thermograms. PCL electrospun fibers in comparison with the respective physical mixtures (PMs), crystalline CAM and carrier

polymer: heating (A) and cooling (B); PCL/PEO electrospun fibers in comparison with the respective PMs, crystalline CAM and carrier polymers: heating (C) and cooling (D);

Key: CAM – chloramphenicol; PCL – polycaprolactone; PEO – polyethylene oxide.

2.3 MD simulation

In both cases, we see no effect on the polymer morphology due to the presence of CAM (Fig. S3).

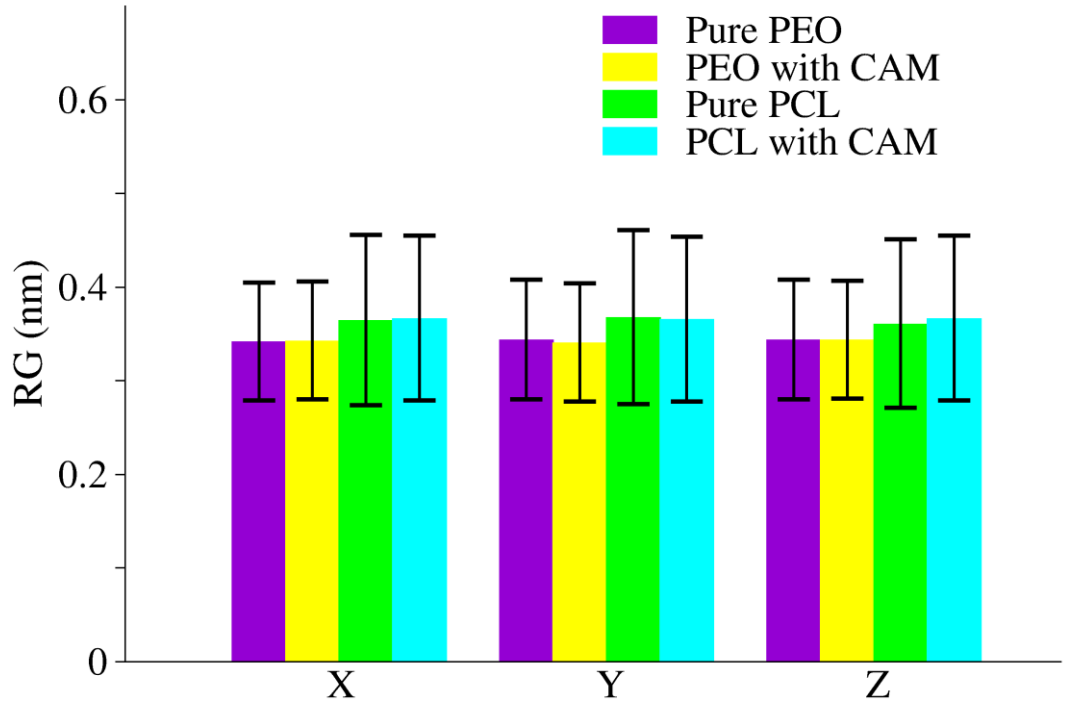

Fig. S3. The x, y and z coordinates of the Radius of gyration calculations for both polymers (PCL and PEO) in absence and presence of CAM. Key: PCL – polycaprolactone; PEO – polyethylene oxide; CAM – chloramphenicol.

References

(1) Jorgensen, W. L.; Tirado-Rives, J. The OPLS [Optimized Potentials for Liquid Simulations] Potential Functions for Proteins, Energy Minimizations for Crystals of Cyclic Peptides and Crambin. *J. Am. Chem. Soc.* **1988**, *110* (6), 1657–1666.

(2) Stepniewski, M.; Pasenkiewicz-Gierula, M.; Róg, T.; Danne, R.; Orlowski, A.; Karttunen, M.; Urtti, A.; Yliperttula, M.; Vuorimaa, E.; Bunker, A. Study of PEGylated Lipid Layers as a Model for PEGylated Liposome Surfaces: Molecular Dynamics Simulation and Langmuir Monolayer Studies. *Langmuir* **2011**, *27* (12), 7788–7798.

(3) Di Pasquale, N.; Marchisio, D. L.; Barresi, A. A.; Carbone, P. Solvent Structuring and Its Effect on the Polymer Structure and Processability: The Case of Water–Acetone Poly-ε-Caprolactone Mixtures. *J. Phys. Chem. B* **2014**, *118* (46), 13258–13267.

(4) Frisch; Trucks, G.; Schlegel, H.; Scuseria, G.; Robb, M.; Cheeseman, J.; Scalmani, G.; Barone, V.; Mennucci, B.; Petersson, G.; Nakatsuji, H.; Caricato, M.; Li, X.; Hratchian, H.; Izmaylov, A.; Bloino, J.; Zheng, G.; Sonnenberg, J.; Hada, M.; Ehara, M.; Toyota, K.; Fukuda, R.; Hasegawa, J.; Ishida, M.; Nakajima, T.; Honda, Y.; Kitao, O.; Nakai, H.; Vreven, T.; Montgomery, J.; Peralta, J.; Ogliaro, F.; Bearpark, M.; Heyd, J.; Brothers, E.; Kudin, K.; Staroverov, V.; Kobayashi, R.; Normand, J.; Raghavachari, K.; Rendell, A.; Burant, J.; Iyengar, S.; Tomasi, J.; Cossi, M.; Rega, N.; Millam, J.; Klene, M.; Knox, J.; Cross, J.; Bakken, V.; Adamo, C.; Jaramillo, J.; Gomperts, R.; Stratmann, R.; Yazyev, O.; Austin, A.; Cammi, R.; Pomelli, C.; Ochterski, J.; Martin, R.; Morokuma, K.; Zakrzewski, V.; Voth, G.; Salvador, P.; Dannenberg, J.; Dapprich, S.; Daniels, A.; Farkas; Foresman, J.; Ortiz, J.; Cioslowski, J.; Fox, D. Gaussian 09, Revision E.01. *Gaussian 09, Revis. B.01, Gaussian, Inc., Wallingford CT* **2013**.

(5) Singh, U. C.; Kollman, P. A. An Approach to Computing Electrostatic Charges for Molecules. *J. Comput. Chem.* **1984**, *5* (2), 129–145.

(6) Bayley, C. I.; Cieplak, P.; Cornell, W.; Kollman, P. A. A Well-Behaved Electrostatic Potential Based Method Using Charge Restraints for Deriving Atomic Charges: The RESP Method. *J. Phys. Chem.* **1993**, *97* (40), 10269–10280.

(7) Wang, J.; Wang, W.; Kollman, P. A.; Case, D. A. Automatic Atom Type and Bond Type Perception in Molecular Mechanical Calculations. *J. Mol. Graph. Model.* **2006**, *25* (2), 247–260.

(8) Case, D. A.; Babin, V.; Berryman, J.; Betz, R.; Cai, Q.; Cerutti, D.; Al., E. AMBER 14. University of California, San Fransisco. University of California, San Francisco 2014.

(9) Berendsen, H.; Grigera, J.; Straatsma, T. The Missing Term in Effective Pair Potentials. *J. Phys. Chem* **1987**, *91* (24), 6269–6271.

(10) Darden, T.; York, D.; Pedersen, L. Particle Mesh Ewald: An $N \cdot \log(N)$ Method for Ewald Sums in Large Systems. *J. Chem. Phys.* **1993**, *98* (12), 10089–10092.

(11) Hess, B.; Bekker, H.; Berendsen, H. J. C.; Fraaije, J. G. E. M. LINCS: A Linear Constraint Solver for Molecular Simulations. *J. Comput. Chem.* **1997**, *18* (12), 1463–1472.

(12) Schaftenaar, G.; Noordik, J. H. Molden: A Pre- and Post-Processing Program for Molecular and Electronic Structures*. *J. Comput. Aided. Mol. Des.* **2000**, *14* (2), 123–134.

(13) Humphrey, W.; Dalke, A.; Schulten, K. VMD: Visual Molecular Dynamics. *J. Mol. Graph.* **1996**, *14* (1), 33–38.

(14) Hubbard, S.; Thornton, J. NACCESS, Computer Program. Department of Biochemistry and Molecular Biology, University College London.

(15) Wang, X.; Zhao, H.; Turng, L. S.; Li, Q. Crystalline Morphology of Electrospun Poly(ε-Caprolactone) (PCL) Nanofibers. *Ind. Eng. Chem. Res.* **2013**, *52* (13).

(16) Elzein, T.; Nasser-Eddine, M.; Delaite, C.; Bistac, S.; Dumas, P. FTIR Study of Polycaprolactone Chain Organization at Interfaces. *J. Colloid Interface Sci.* **2004**, *273* (2), 381–387.

(17) Yang, T.; Sun, X.; Ren, Z.; Li, H.; Yan, S. Crystallizability of Poly(ε-Caprolactone) Blends with Poly(vinylphenol) under Different Conditions. *Chinese J. Polym. Sci.* **2014**, *32* (9), 1119–1127.

(18) Abdelrazek, E. M.; Hezma, A. M.; El-khodary, A.; Elzayat, A. M. Spectroscopic Studies and Thermal Properties of PCL/PMMA Biopolymer Blend. *Egypt. J. Basic Appl. Sci.* **2016**, *3* (1), 10–15.

(19) Rocco, A. M.; da Fonseca, C. P.; Pereira, R. P. A Polymeric Solid Electrolyte Based on a Binary Blend of Poly(ethylene Oxide), Poly(methyl Vinyl Ether-Maleic Acid) and LiClO4. *Polymer (Guildf).* **2002**, *43* (13), 3601–3609.

(20) Oliveira, J. E.; Mattoso, L. H. C.; Orts, W. J.; Medeiros, E. S. Structural and Morphological Characterization of Micro and Nanofibers Produced by Electrospinning and Solution Blow Spinning : A Comparative Study. **2013**, *2013*.

(21) Si, M. Z.; Kang, Y. P.; Zhang, Z. G. Surface-Enhanced Raman Scattering (SERS) Spectra of Chloramphenicol in Ag Colloids Prepared by Microwave Heating Method. *J. Raman Spectrosc.* **2009**, *40* (9), 1319–1323.

(22) Sajan, D.; Sockalingum, G. D.; Manfait, M.; Hubert Joe, I.; Jayakumar, V. S. NIR-FT Raman, FT-IR and Surface-Enhanced Raman Scattering Spectra, with Theoretical Simulations on Chloramphenicol. *J. Raman Spectrosc.* **2008**, *39* (12), 1772–1783.

(23) Peña, J.; Corrales, T.; Izquierdo-Barba, I.; Doadrio, A. L.; Vallet-Regí, M. Long Term Degradation of Poly(??-Caprolactone) Films in Biologically Related Fluids. *Polym. Degrad. Stab.* **2006**, *91* (7), 1424–1432.

(24) Xu, X.; Wang, H.; Jiang, L.; Wang, X.; Payne, S. A.; Zhu, J. Y.; Li, R. Comparison between Cellulose Nanocrystal and Cellulose Nanofibril Reinforced Poly(ethylene Oxide) Nanofibers and Their Novel Shish-Kebab-like Crystalline Structures. *Macromolecules* **2014**, *47* (10), 3409–3416.

(25) Zoppi, R. a.; Duek, E. a. R.; Coraça, D. C.; Barros, P. P. Preparation and Characterization of Poly (L-Lactic Acid) and Poly(ethylene Oxide) Blends. *Mater. Res.* **2001**, *4* (2), 117–125.

(26) Lowery, J. L.; Datta, N.; Rutledge, G. C. Effect of Fiber Diameter, Pore Size and Seeding Method on Growth of Human Dermal Fibroblasts in Electrospun Poly(ε-Caprolactone) Fibrous Mats. *Biomaterials* **2010**, *31* (3), 491–504.